Chemosphere 270 (2021) 128658

Contents lists available at ScienceDirect

Chemosphere

journal homepage: www.elsevier.com/locate/chemosphere

Multidecadal records of microplastic accumulation in the coastal sediments of the East China Sea

Jia Lin [a], Xiao-Ming Xu [b], Bei-Ying Yue [a], Xiang-Po Xu [a], Jin-Zhong Liu [c], Qing Zhu [a, **], Jiang-Hai Wang [a, d, *]

[a] Guangdong Provincial Key Laboratory of Marine Resources and Coastal Engineering, School of Marine Sciences, Sun Yat-Sen University, Zhuhai, 519082, China
[b] Guangdong Eco-engineering Polytechnic, Guangzhou, 510520, China
[c] Guangzhou Institute of Geochemistry, Chinese Academy of Sciences, Guangzhou, 510640, China
[d] Southern Laboratory of Ocean Science and Engineering (Guangdong, Zhuhai), Zhuhai, 519000, China

HIGHLIGHTS

- A multidecadal increasing trend of microplastic accumulation was revealed in sediment cores in the ECS since the 1960s.
- High abundances of microplastics were detected in the form of fragments with the prevalent size of <100 μm.
- Microplastic accumulation in sediments in the ECS is associated with Chinese plastic production and consumption.
- Microplastics have made an insignificant but potentially-increasing contribution to sedimentary carbon storage in the ECS.

GRAPHICAL ABSTRACT

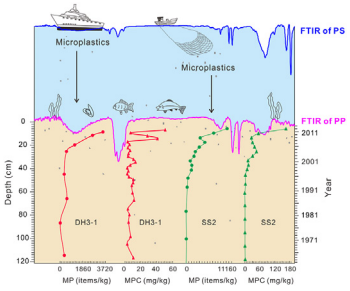

ARTICLE INFO

Article history:
Received 20 August 2020
Received in revised form
12 October 2020
Accepted 15 October 2020
Available online 17 October 2020

Handling Editor: J. de Boer

Keywords:
Microplastic
The East China Sea
Sediment core
Historical accumulation
Carbon storage

ABSTRACT

Microplastics are an emerging hazard in the marine environment, and considered to eventually sink into sediments. An investigation into the long-term variation of microplastic accumulation in sediment cores is essential for understanding the historical trend of this contamination and its response to human activities. In this study, the multidecadal changes of microplastic abundances in two sediment cores from the inner shelf of the East China Sea (ECS) were revealed by two methods, i.e., a visual enumeration method based on scanning electron microscopy-energy dispersive X-ray spectroscopy (SEM-EDS) and a quantitative method based on microplastic-derived carbon (MPC) abundances. The features of microplastics were determined via SEM-EDS and micro-Fourier transform infrared spectroscopy (μ-FTIR). The results reveal a multidecadal increasing trend of microplastic accumulation in the coastal sediments of the ECS since the 1960s, which may be jointly governed by the release of plastic wastes and oceanographic dynamics. Meanwhile, the breakpoint of the exponential growth of microplastics in the ECS occurs in 2000 AD, which well matches the rapid increasing of plastic production and consumption in China. Further, based on the MPC contents in sediments, the influence of microplastics on the

* Corresponding author. Guangdong Provincial Key Laboratory of Marine Resources and Coastal Engineering, School of Marine Sciences, Sun Yat-Sen University, Zhuhai, 519082, China.
** Corresponding author.
E-mail addresses: zhuq36@mail.sysu.edu.cn (Q. Zhu), wangjhai@mail.sysu.edu.cn (J.-H. Wang).

https://doi.org/10.1016/j.chemosphere.2020.128658

quantitative evaluation of carbon storage in the ECS has been examined for the first time, revealing an insignificant (<2% before 2014 AD) but potentially-increasing (6.8% by 2025 AD) contribution of microplastics to carbon burial. Our results may provide the important data for evaluating and mitigating the impact of microplastics on the marine environment.

1. Introduction

Microplastics (<5 mm in diameter) are ubiquitous in the marine environment, and have been identified as emerging contaminants regarding their adverse ecological impacts (Thompson et al., 2004; Rochman et al., 2013; Nguyen et al., 2019). Microplastic ingestion by marine animals at different trophic levels has been documented in numerous researches (Wang et al., 2019; Bagheri et al., 2020; Hossain et al., 2020). It has been confirmed that microplastic ingestion can cause the blockage of alimentary canals, inflammation, growth retardation, impaired reproduction, and even death to organisms (Cole et al., 2015; Jovanović, 2017). The uptake of microplastics may also result in toxic contaminants entering the marine ecosystem, because microplastics as an efficient adsorbent can absorb and concentrate persistent organic pollutants and heavy metals from their ambient seawater (Law and Thompson, 2014; Turner and Holmes, 2015). Further, microplastics may also release harmful additives such as phthalates and flame retardants, which may disrupt the endocrine system of animals (Law and Thompson, 2014; Seyoum and Pradhan, 2019).

Marine sediment is a final sink for microplastics (Browne et al., 2011; Woodall et al., 2014). To better manage this pollutant, many efforts have been made for monitoring the abundance, distribution and dynamic accumulation of microplastics in sediments (Willis et al., 2017; Wang et al., 2019; Su et al., 2020). Recent studies suggest that the multidecadal records of microplastics in sediment cores are significant to fully unravel their dynamic accumulation in sediments in the absence of long-term monitoring (Brandon et al., 2019; Turner et al., 2019; Li et al., 2020). For example, based on the historical change of microplastics between 1740s and 2000s in sediment cores from an estuary in Tasmania, Australia, Willis et al. (2017) found that microplastic accumulation in sediments was closely associated with the growing plastic production, urban effluent, and scouring events. Brandon et al. (2019) revealed the microplastic variation in a sediment core spanning a period of 1834–2009 AD in the Santa Barbara Basin, California, and predicted a continuously increasing tendency of microplastic accumulation in future. However, most of the previous efforts on microplastic accumulation have merely focused on surface sediments, and the studies on the time series of microplastics in sediment cores are still insufficient (Matsuguma et al., 2017; Willis et al., 2017; Fan et al., 2019).

Except the impact on ecosystems, microplastic accumulation in sediments is also related to other environmental issues such as marine carbon storage (Rillig, 2018; Yu et al., 2019; Rillig and Lehmann, 2020). It is generally appreciated that marine carbon storage largely influences marine carbon cycling and global climate change (Schuur et al., 2015; Talley et al., 2016). However, microplastic accumulation in marine sediments may lead to an overestimation of carbon storage, because these carbon-dominated anthropogenic materials are incorporated into total organic carbon (TOC) and can make a hidden contribution to carbon burial (Rillig, 2018; Rillig and Lehmann, 2020). Rillig (2018) suggested that the microplastic-derived carbon (MPC) may account for at least 0.1%–5% of the TOC in terrestrial soils. However, such a contribution should be distinguished in the evaluation of carbon cycling, because microplastics are artificial organic materials with different functions in comparison with natural ones. Nevertheless, the contribution of microplastics to carbon sequestration in the marine system has not been quantified up to date.

The East China Sea (ECS) is a marginal sea of the Pacific Ocean, which borders the densely populated and industrialized center in eastern China. The ECS has been recognized as the area with a heavy microplastic contamination due to the massive effluent discharge as well as the frequent maritime and fishery activities (Zhang et al., 2019a). The occurrence of microplastics in sediments has been revealed from estuaries to offshore areas (Peng et al., 2017; Zhang et al., 2019a). Further, the fine-grained sedimentary area in the ECS provides sediment cores with continuous sedimentary sequences, which may excellently record the long-term deposition of pollution (Lin et al., 2018), including microplastics. In this study, two centennial-scale sediment cores were collected from the coastal fine-grained sedimentary zone in the ECS for exploring the temporal change of microplastics. Factors involved in microplastic accumulation in sediments were accordingly discussed, and the contribution of microplastics to carbon storage in two cores was also examined. Our results not only provide the important data for assessing microplastic pollution in the benthic ecosystem, but also reveal their contribution to marine carbon burial.

2. Materials and methods

2.1. Background and sampling

The ECS is bounded by mainland China on the west and by the Okinawa Trough on the east, covering an area of 1.25×10^6 km^2 (Fig. 1). The ECS is characterized by complex hydrodynamic conditions, mainly affected by the Changjiang River Plume, the Taiwan Warm Current, the East China Sea Coastal Current, the Kuroshio Current, tides, and wind-driven waves (Fig. 1) (Lin et al., 2019). The Changjiang River discharge supplies the bulk of suspended matters in the ECS (Pang et al., 2016). Under the integrated influence from the complex hydrodynamic and massive river discharge, a fine-grained sedimentary belt with a sediment thickness of 0–40 m was formed in the coastal area off Fujian and Zhejiang Provinces, termed as the Min-Zhe fine-grained sedimentary zone (Fig. 1) (Liu et al., 2009; Lin et al., 2018).

Two sediment cores (DH3-1: 122.5000°E, 30.0000°N; and SS2: 121.2907°E, 27.5089°N) were collected from the Min-Zhe fine-grained sedimentary zone using a gravity corer in the summer of 2012 and winter of 2014, respectively (Fig. 1). Cores DH3-1 and SS2 are 7 cm in diameter and 45 cm and 313 cm in length, respectively. After collection, both cores were sealed in clean polyvinyl chloride (PVC) tubes, and stored at −20 °C until analysis. Then, the cores were respectively sectioned at the intervals of 0.5 cm (core DH3-1) and 2 cm (core SS2) on the basis of their sedimentation rates as revealed by Lin et al. (2018) and Wang et al. (2018).

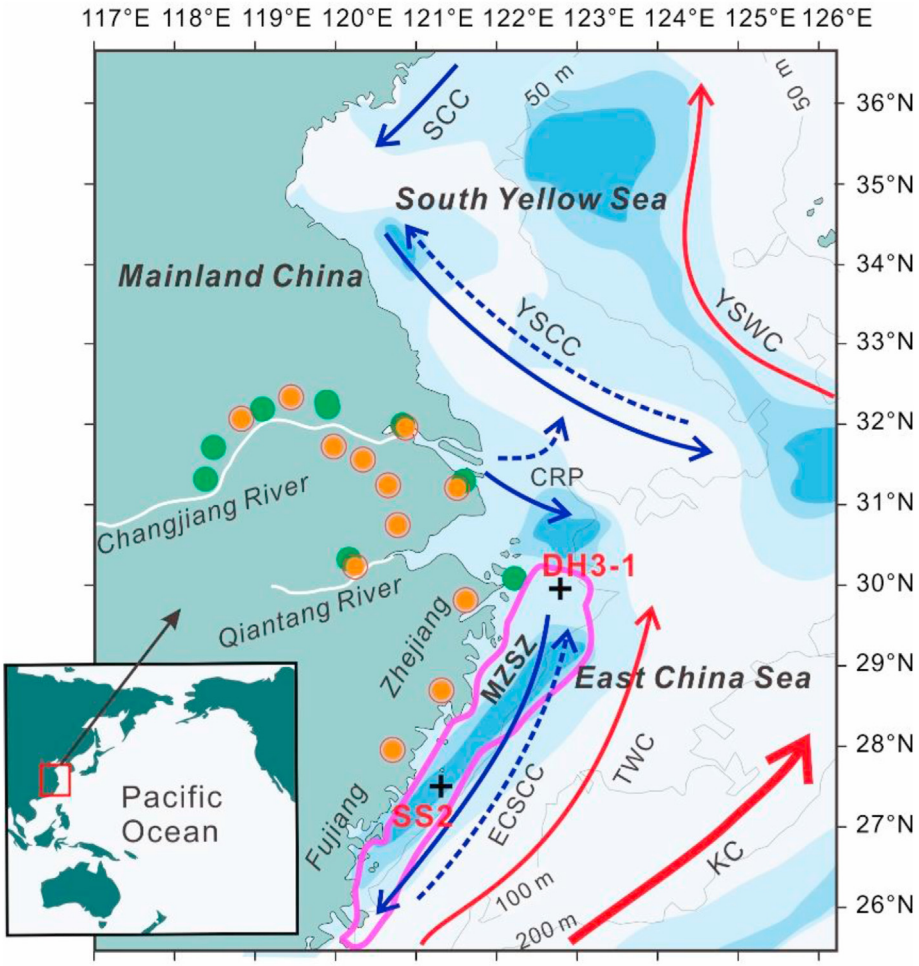

Fig. 1. Schematic map illustrating the background of the East China Sea and locations of sediment cores DH3-1 and SS2 in the Min-Zhe sedimentary zone (MZSZ, solid line in purple). Large harbors and cities are marked by green and orange dots, respectively. The areas of argillaceous sediments are shaded in blue, and the darker colors represent finer-grained sediments. The solid red and blue arrows denote warm and cool currents, respectively. KC, Kuroshio Current; TWC, Taiwan Warm Current; ECSCC, East China Sea Coastal Current; CRP, Changjiang River Plume; YSCC, Yellow Sea Coastal Current; YSWC, Yellow Sea Warm Current; and SCC, Shandong Coastal Current. The dashed arrows represent the summer patterns of the YECC, CRP, and ECSCC (modified according to Lin et al., 2019). (For interpretation of the references to color in this figure legend, the reader is referred to the Web version of this article.)

2.2. Determining the abundances of microplastics

Two quantification methods were employed for determining the abundances of microplastics in subsamples, i.e., counting microplastic items via scanning electron microscopy and detecting MPC contents.

2.2.1. Enumerating microplastics

Eight (1971–2009 AD) and sixteen (1942–2012 AD) subsamples from cores DH3-1 and SS2 were selected for enumerating their microplastic items, respectively. Briefly, after dried, 10–20 g of each subsample was treated with Fenton's reagent at room temperature for 2 h before being heated to 70 °C for 45 min for digesting organic matters. Each digested subsample was dried and then mixed with 100 mL of a sodium iodide solution (NaI, 1.60 g/cm^3). The mixture was stirred for 2 min, treated by ultrasonic waves for 5 min, and then left to sit for 2 h. Subsequently, about 30 mL of the topmost supernatant was filtered through a mixed fiber filter (MFF) paper with the pore size of 2 μm (Xinya, Shanghai, China) for extracting and concentrating microplastics. This extraction step was performed in triplicate. The obtained filter papers were then introduced into clean Petri dishes and dried at 50 °C overnight.

The field emission environmental scanning electron microscopy (FEI, Hillsboro, OR, USA) coupled with an energy-dispersive X-ray spectroscopy (Oxford, Bucks, UK) (SEM-EDS) was used to count and characterize the extracted microplastics. Three parts with the respective area of 5 mm × 12 mm were cut from each filter paper, and gilded for SEM-EDS analysis. Working conditions of the SEM-EDS were described as below: working distance, 10 mm; accelerating voltage, 20 kV; and resolutions for SEM, 2.0 nm (30 kV) and 3.5 nm (3 kV). Under the SEM-EDS, suspected particles were counted as microplastics if they met the following criteria: (1) no structure of organic materials (such as cell wall) is visible; (2) carbon is the only major element; or carbon and chlorine are the major elements for PVC particles; and (3) fiber is evenly thick with dots, holes or streaks on its surface, and no segmented structure; or appears as a bent/twisted flat ribbon (Nor and Obbard, 2014; Wang et al., 2017; Zhu et al., 2019).

2.2.2. Quantifying MPC contents

As microplastics are carbon-dominated matters, microplastics may be quantified via determining the MPC contents in samples after an efficient concentration and purification (including the removal of inorganic and other organic carbon). In this study, a

newly-developed method was employed for detecting the MPC contents in sediments. Twenty-eight (1966–2010 AD) and twenty-one (1938–2013 AD) subsamples from cores DH3-1 and SS2 were selected for measuring their MPC contents, respectively. For each subsample, 10−30 g of the dried sediment was used. Briefly, after the digestion of organic matters with Fenton's reagent, microplastics were extracted using a NaI solution (1.60 g/cm^3); and the extracted microplastics were filtrated onto grass fiber filter (GFF) papers with the pore size of 0.22 μm (Xinya, Shanghai, China). The steps of digestion and extraction were the same as those described above. Each obtained GFF paper was then introduced into a disposable ceramic crucible with micropores (Liling Chashan Crucible Factory, Hunan, China) and dried at 50 °C for 3 h. Subsequently, about 2 mL of >85% phosphoric acid was added into the crucible for removing inorganic carbon such as carbonates. After that, an elution step was conducted with ultrapure water and repeated six times for washing off the residual acid. The GFF papers were then dried at 50 °C overnight. Finally, the MPC content of each subsample was measured by an ELTRA CS 800 carbon-sulfur analyzer (ELTRA, Haan, Germany). Details on the validation of this method are presented in Supplementary material 1.

2.3. Characterizing microplastics

The morphological characteristics of every microplastic particle, including shape, size and surface microstructure were simultaneously observed under the SEM-EDS. The sizes of microplastics were measured by the maximum width. It should be noted that, as individual fiber is always bent or twisted, the sizes of fibers were determined by their overall size instead of their total length. Additionally, about 12% of suspected microplastics were randomly selected for identifying their polymer types using the Fourier transformation infrared spectrometer coupled with a microscope (μ-FTIR) (Thermo Fisher Scientific, Waltham, MA, USA) in the transmission mode or attenuated total reflectance mode. This subset of suspected microplastics was selected from 22 subsamples, which represented various shapes and colors in the wide size range of 300−5000 μm. The FTIR spectrum of each particle was collected in a spectral range of 650−4000 cm^{-1}, at a resolution of 4 cm^{-1}, and in an acquisition time of 60 s with 64 co-scans. After performing the baseline correction, the obtained spectra were compared with the standard polymer spectra in libraries using software OMNIC (Thermo Fisher Scientific, Waltham, MA, USA); and polymer types of microplastics were accordingly determined. Results of FTIR analyses were further used to adjust the concentrations of microplastics.

2.4. Contamination prevention and blank test

To prevent contamination, all instruments were rinsed with pure water and dried before use. Plastic instruments were avoided if possible. Cotton laboratory coats and latex gloved hands were worn during the sample treatment. Also, during subsampling, the outermost 2 mm of sediments in contact with the PVC tube were discarded to exclude external PVC particles. The sample pretreatment was performed in a clean fume hood; and processing samples were covered with aluminum foils. When running each batch of samples, we simultaneously performed blank tests ($n = 3$) for calibrating their background values in the microplastic enumeration and MPC measurement.

2.5. Total organic carbon analysis of the sediments

Twenty-seven and eighteen subsamples from cores DH3-1 and SS2 were taken for determining their TOC contents, respectively, via the method of Xu et al. (2018). Briefly, all subsamples were freeze-dried and manually grounded to a size of <100 μm. Approximately 100 mg of each subsample was introduced into a semi-permeable ceramic crucible, and treated with 3 mol/L of hydrochloric acid to eliminate carbonates. Finally, their TOC contents were determined by a CS230C/S analyzer (LECO, St. Joseph, MO, USA).

2.6. Other data sources and data processing

Based on the published ^{210}Pb dating result (Lin et al., 2018), the chronological sequence of core SS2 was established by comparing the periodical time series of black carbon contents between cores SS2 and DH5-1 (122.1845°E; 28.4360°N) in the inner shelf of the ECS (The detailed information of black carbon time series in two cores are illustrated in Fig. S1). The chronological sequence in core DH3-1 was determined according to the regional sedimentation rate of 1 cm/year (Wang et al., 2018). The data of annual plastic production in China were cited from Song (1993) and the National Bureau of Statistics of China (http://data.stats.gov.cn/index.htm). All the data processing was performed in Excel Professional Plus 2016 (Microsoft, Redmond, WA, USA) and Prism 8 (Graphpad, San Diego, CA, USA). The relationship between microplastic abundance and Chinese plastic production was analyzed using Pearson's product-moment correlation. A one-factor ANOVA test was performed for these data, and the statistical significance was set at $\alpha = 0.05$.

3. Results

3.1. Assessment of procedural blanks

To ensure the reliability of results, the measures for quality control were strictly adopted during the sample treatment for preventing contamination (Prata et al., 2020). An average of 5.0 (±1.0) fibers per sample was found in the blank test for microplastic enumeration; while a mean of 0.03 (±0.02) mg C per measurement was yielded in the procedural blanks for the MPC detection. These values were subsequently used to adjust the measured results of microplastic concentrations and MPC contents.

3.2. Microplastic abundances

The abundances of microplastic items for cores DH3-1 and SS2 are listed in Tables S1 and 2. The total numbers of 70 and 383 microplastics were observed in 7 subsamples from core DH3-1 and 15 subsamples from core SS2, respectively. The microplastic abundances in core DH3-1 vary at the interval of 0−2378 items/kg dry weight (dw), with an average of 366 items/kg dw (1971–2009 AD); while the microplastic concentrations in core SS2 range from 0 items/kg dw to 7746 items/kg dw, with a mean of 653 items/kg dw (1942–2012 AD). As shown in Fig. 2, the microplastic abundances in cores DH3-1 and SS2 exhibit obviously increasing trends since the 1960s. In particular, microplastics clearly accumulated in the top sections of both sediment cores corresponding to the period after 2000 AD.

The MPC data for cores DH3-1 and SS2 are presented in Tables S3 and 4, and their variations are shown in Fig. 2. It can be seen that the MPC contents in core DH3-1 range from 2.75 mg/kg dw to 50.57 mg/kg dw with a mean of 8.21 mg/kg dw (1966–2010 AD); whereas the MPC contents in core SS2 are at the interval of 0−165.39 mg/kg dw with an average of 8.48 mg/kg dw (1938–2013 AD). As shown in Fig. 2, there are evidently increasing trends in the MPC contents in both cores since the 1960s. Particularly, the enhanced MPC accumulation occurs in the topmost 11 cm and

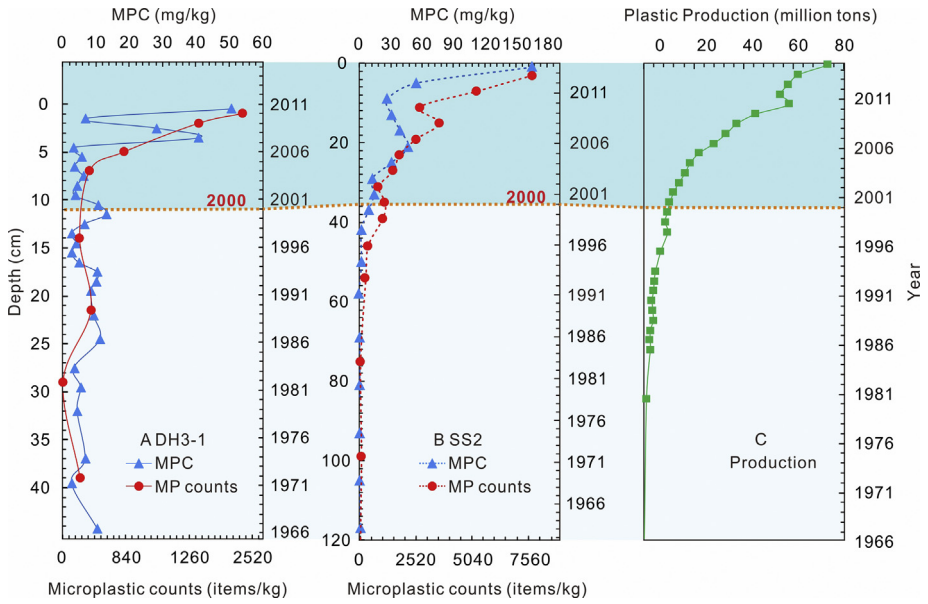

Fig. 2. Time series of the abundances of microplastic items and microplastic-derived carbon (MPC) contents in sediment cores DH3-1 (A) and SS2 (B) in comparison with the annual plastic production (in primary forms) in China (C).

36 cm of cores DH3-1 and SS2, respectively, being equivalent to the period after 2000 AD. Such increasing trends well match those of the abundances of microplastic items. Significant correlations (r = 0.9595 and 0.9222 for cores DH3-1 and SS2, respectively; $p < 0.05$) are yielded between the time series of MPC contents and microplastic numbers (Fig. S2).

3.3. Characteristics of microplastics

Microplastics occur in various shapes, including fragments, fibers, films, and quasi-spherical particles. Overall, fragments are the most prominent plastic particles, accounting for 73.58% and 50.55% of the total microplastics in cores DH3-1 and SS2, respectively, followed by fibers, quasi-spherical particles, and films (Fig. 3A). In core SS2, microplastic fibers dominate their shape in the lower section (>35 cm) corresponding to the period before 2000 AD; whereas fragments become the most prevalent shape in the upper section deposited after 2000 AD (<35 cm) (Fig. 3B). In contrast, the fragments are predominant in subsamples throughout core DH3-1 (Fig. 3C).

Microplastics were categorized into five size ranges, i.e., <50 μm, 50–100 μm, 100–300 μm, 300–1000 μm, and 1000–5000 μm. As illustrated in Fig. 3D, the microplastic abundances increase with declining size. Overall, the finest fraction with the size of <50 μm is

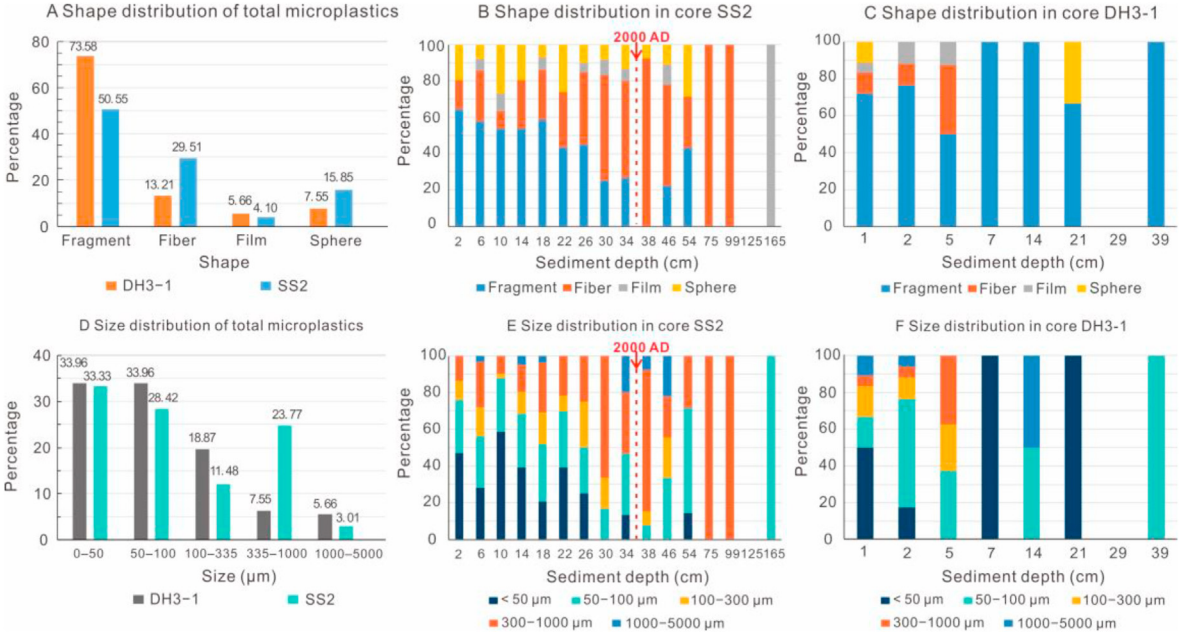

Fig. 3. Shape and size distributions of the total microplastics in cores DH3-1 (n = 70) and SS2 (n = 383) (A–B), and the shape and size distributions of microplastics in each subsample from the two cores (C–F). Microplastics were not found from the subsamples at the depths of 29 cm in core DH3-1 and 125 cm in core SS2.

most prevalent, accounting for 33.96% and 33.33% of the total microplastics in cores DH3-1 and SS2, respectively. Specifically, microplastics with the size of >100 μm in core SS2 are the most abundant in its lower section (<35 cm) deposited before 2000 AD; while microplastics with the size of <100 μm become dominant in the upper section (Fig. 3E). For core DH3-1, microplastics with the size of <100 μm are the most common particles in all subsamples (Fig. 3F).

Fifty suspected particles (including 41 non-fibrous particles and 9 fibers) were randomly selected for μ-FTIR analysis; and 21 of them were confirmed as fully synthetic polymers, and 10 as cellophanes or celluloses. Because cellophane as a regenerated cellulosic material reflects different production and degradation paths with other plastic materials, it is excluded from microplastics in our result (Comnea-Stancu et al., 2017; Stark, 2019; Suaria et al., 2020). Therefore, the success rate of microplastic identification in this study was 42.0%, which has been used to adjust microplastic concentrations. Six synthetic polymers were identified, including polypropylene (PP), polyethylene (PE), polystyrene (PS), polyethylene terephthalate (PET), PVC, and PP-PE copolymer (Fig. 4A–F). Thereinto, PP dominates the polymer types with a proportion of 28.57%, followed by PS (23.81%), PET (19.05%), PE (14.29%), PVC (9.52%), and PP-PE (4.75%). As for cellulosic materials, cellophane and cellulose share the fractions of 60.00% and 40.00%, respectively (Fig. 4G–H). Also, the influence of cellulosic fibers on the MPC measurement was discussed in Supplementary material 2, indicating a general insignificant effect.

High resolution images of the extracted microplastics were taken via a SEM-EDS (Fig. 4I–K), and the morphological characteristics of plastic particles were observed. It can be seen that most microplastics exhibit uneven, cracked, and even porous surfaces (Fig. 4I–J), indicating the ongoing weathering and fragmentation. Some smaller particles derived from larger microplastics exhibit relatively smooth surfaces (Fig. 4I and K).

3.4. MPC proportions in the TOC

The TOC contents and MPC/TOC ratios for cores DH3-1 and SS2 are presented in Tables S5 and 6. It is clear that the TOC concentrations in core DH3-1 range from 0.24% to 0.80% with an average of 0.51%; while the TOC values in core SS2 are at the interval of 0.41–0.60% with a mean of 0.48%. The MPC/TOC ratios vary between 0.04 and 0.51% (core DH3-1) and 0–1.32% (core SS2), with an MPC/TOC mean of 0.18%. The highest MPC proportions in the TOC occur in the topmost of both cores.

4. Discussion

4.1. Comparison of microplastic abundances

Microplastic pollution in the marine system is a pressing issue. The ECS has been identified as an area which is susceptible to microplastic contamination (Peng et al., 2017; Zhang et al., 2019a, b). In this study, relatively high abundances of microplastics are observed in the coastal sediments of the ECS, with the maximum of 7746 items/kg dw in core SS2. The concentration of microplastics in the surface sediments (0–5 cm) is 1591 items/kg dw in core DH3-1, which is much higher than those in the sediments of the Changjiang Estuary (Peng et al., 2017), the offshore area in the ECS (Zhang et al., 2019a), the Mediterranean Sea (Alomar et al., 2016), and the French Atlantic coast (Phuong et al., 2018), but close to those in the South Yellow Sea (Wang et al., 2019), the Venice lagoon, Italy (Vianello et al., 2013) and the Halifax harbor, Canada (Mathalon and Hill, 2014) (Table 1). In contrast, the surface sediment in core SS2 has a higher microplastic abundance (7120 items/kg dw), which is significantly higher than those in the ECS (240 items/kg dw) reported by Zhang et al. (2019a).

The discrepancy in microplastic concentrations in the ECS between this study and previous researches may result from the heterogeneous distribution of microplastics or more importantly, the different methods for enumerating microplastics. In general, microplastics are previously quantified via manual counting under optical microscopes, which is inadequate to identify very fine particles (<50 μm) (Table 1) and thus prone to errors (Hanvey et al., 2017; Nel et al., 2019). In this study, the SEM-EDS with a resolution of 2 nm was employed for enumerating the very fine microplastics and simultaneously distinguishing these particles from other non-plastic particles according to their elemental compositions. Our results show that microplastics with the size of <50 μm account for >30% of the total plastic particles, but which are usually ignored in many previous studies (Peng et al., 2017; Wang et al., 2019; Xue et al., 2020) (Table 1). Furthermore, it is difficult to identify plastic fragments through visual observations under optical microscopes, due to the similarity in their appearances between plastic fragments and non-plastic particles, especially for small fragments (Fischer and Scholz-Bö;ttcher, 2017). In this study, the SEM equipped with a back-scattered electron (BSE) detector was used for sample imaging, under which microplastic fragments looked evidently darker than other mineral particles, and thus can be quickly identified. Therefore, more microplastic fragments were found in the studied sediments in comparison with those in previous studies (Peng et al., 2017; Zhang et al., 2019a; Zheng et al., 2019) (Table 1). Further, the actual concentrations of microplastics have been corrected on the basis of the μ-FTIR analyses. Thus, the high abundances of microplastics measured by a SEM-EDS are reliable in this study.

Additionally, another method was used to determine microplastic abundances by measuring the MPC contents in samples. As presented in Fig. 2, similar temporal variation trends of the MPC contents and microplastic abundances are observed in both cores, with a significant correlation ($r > 0.9$, $p < 0.05$) (Fig. S2), which may indicate the validity of the two methods and high-quality of the data obtained in this study.

4.2. Historical variation of microplastic accumulation in sediments

4.2.1. Anthropogenic activities promoting microplastic accumulation

The vertical variations of microplastic abundances in two cores have revealed a multidecadal increasing trend of microplastic accumulation in coastal sediments in the ECS since the 1960s (Fig. 2). This increasing trend is similar with those in the Irish Continental Shelf (Martin et al., 2017), the Derwent Estuary, Australia (Willis et al., 2017), the Santa Barbara Basin, California (Brandon et al., 2019), and Hangzhou Bay, China (Li et al., 2020).

Comparative analysis suggests that the microplastic deposition in the ECS is significantly correlated with the plastic production in China ($r = 0.7084$ and 0.9573 for cores DH 3-1 and SS2, respectively; $p < 0.05$) (Table S7; Fig. 2C). This significant correlation indicates that the accelerated growth of plastic production and consumption has directly enhanced the input of plastic wastes and particles into the ECS, which exacerbates microplastic accumulation in downstream sediments (Browne et al., 2011; Eriksen et al., 2013). Specifically, owing to the limited prevalence of plastic products in China before the 1980s, low abundances of microplastics have been accordingly observed (106.02 items/kg dw and 20.99 items/kg dw for cores DH3-1 and SS2, respectively) in the 1960s and 1970s. Microplastic abundances in the 1980s and 1990s steadily increase up to 220.43 items/kg dw and 412.20 items/kg dw in cores DH3-1 and SS2, respectively, which corresponds to the

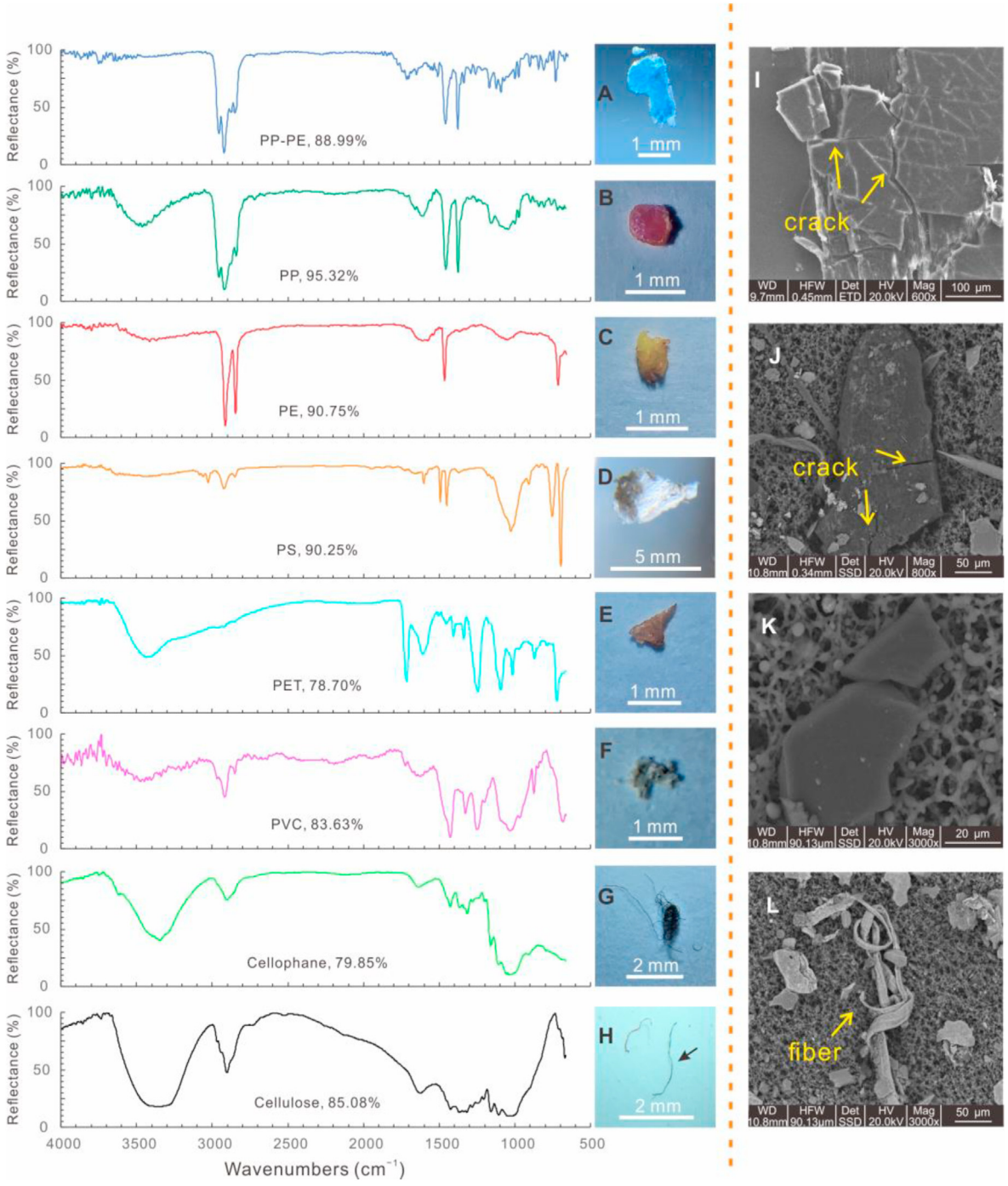

Fig. 4. Infrared spectra and microphotographs of the most frequently observed microparticles and cellulosic fibers. A, Polypropylene-polyethylene (PP-PE) fragment; B, Polypropylene (PP) pellet; C, Polyethylene (PE) fragment; D, Polystyrene (PS) fragment; E, Polyethylene terephthalate (PET) fragment; F, Polyvinyl chloride (PVC) film; G, Cellophane; and H, Cellulose. I to L, Scanning electron microscope (SEM) images of the extracted microplastics.

stable development of plastic production in China. The year of 2000 AD is an important breakpoint of the exponential microplastic accumulation, which coincides exactly with the rapid growth of plastic production in China.

In addition, microplastic fibers are dominant in core SS2 before the 2000s; while fragments dominate microplastics after 2000 AD (Fig. 3). This temporal increase of fragments agrees with those observed in the sediments from the urban lake in London, UK (Turner et al., 2019) and the Santa Barbara Basin, California, US (Brandon et al., 2019). Fibers were largely derived from domestic effluents (Browne et al., 2010; Mintenig et al., 2017); whereas fragments in this study were originated from the degradation of larger plastic wastes (Fig. 4). The shape change of microplastics in core SS2 may demonstrate that the domestic effluent is their dominant source before 2000 AD; while the leakages of plastic litters from industrial, domestic, agriculture and aquaculture sources are their main origin after 2000 AD. The above conclusion well matches the rapid development of industry and agriculture after 2000 AD in China. In contrast, fragments are the most abundant shape of plastic particles in core DH3-1, suggesting their

Table 1
Comparison of microplastic abundances in surface sediments between the East China Sea (ECS) and other coastal areas.

Location	Quantification strategy	Magnification factor	MP Abundance (items/kg dw)	Size (μm)	Dominant shape	Reference
Changjiang Estuary, China	Dissecting microscope	–	20–340	46–4968	Fiber	Peng et al. (2017)
Beach of the south china sea	Fluorescence microscope	100	5014–8714	–	Fiber	Qiu et al. (2015)
North Yellow Sea	Stereomicroscope	–	37–123	>30	Film and fiber	Zhao et al. (2018); Zhu et al. (2018)
Offshore area in ECS, China	Stereomicroscope	160	60–240	19–4953	Fiber	Zhang et al. (2019a)
South Yellow sea	Stereomicroscope	–	560–4205	>50	Fiber	Wang et al. (2019)
Beibu Gulf, South China Sea	Stereomicroscope	50	20–1200	>100	Fiber	Xue et al. (2020)
Lagoon of Venice, Italy	Optical microscope	–	672–2175	30–1000	Fragment	Vianello et al. (2013)
Halifax Harbor, Nova Scotia, Canada	Dissecting microscope	2	2000–8000	–	Fiber	Mathalon and hill. (2014)
Khark Island, Iran	Binocular microscope	200	295–1085	–	Fragment	Akhbarizadeh et al. (2017)
Mediterranean Sea	Stereomicroscope	6–40	100–900	>63	Fiber	Alomar et al. (2016)
French Atlantic coast	Optical microscope	160	38–102	40–2000	Fragment	Phuong et al. (2018)
Hiroshima Bay, Japan	Stereomicroscope	–	24–253	>300	Complex shape	Sagawa et al. (2018)
Inner shelf of ECS, China	SEM-EDS	7–10^6	1591–7120	12–4890	Fragment	This study

Note: SEM-EDS, scanning electron microscopy-energy-dispersive X-ray spectroscopy; FTIR, Fourier transform infrared spectroscopy; Raman, Raman spectroscopy.

source from the degradation of macroplastics. In comparison with core SS2, the variation of microplastic types in core DH3-1 is inconsistent with the historical change of plastic consumption and development, which may result from the different hydrodynamic environments at the two sampling sites as explained in section 4.2.2.

In the studied sediments, PP, PS and PET are the most prevailing polymers in microplastics, which are accordant with their widespread use in China (Ma et al., 2019). PP, PS and PET are extensively utilized as packing and industrial materials. PP is also frequently used in agriculture and fishery industry. The pervasiveness of PP, PS and PET microplastics indicates the recent mismanagement of plastic wastes and plastic-bearing effluents in the reaches of the Changjiang River.

4.2.2. Hydrodynamics influencing microplastic accumulation

Once in seawater, the fate of microplastics is inevitably influenced by hydrodynamics (Isobe et al., 2015; Jiang et al., 2020). In this study, the concentrations of microplastic particles in core SS2 are higher than those in core DH3-1, which may be attributed to the hydrodynamic condition in the ECS (Fig. 1). Core DH3-1 was collected from the Changjiang River Estuary with a high-energy hydrodynamic condition, mainly affected by the Changjiang River Plume, the ECS Coastal Current, and the Taiwan Warm Current (Fig. 1). In this environment, most of the suspended microplastics are likely removed from this region by the Changjiang River Plume and the Coastal Current (Zhang et al., 2020). Comparatively, core SS2 was taken from the middle segment of the Min-Zhe fine-grained sedimentary zone (Fig. 1), which is less subject to intense hydrodynamic forces. Due to the coupling between the ECS Coastal Current and Taiwan Warm Current, microplastics are allowed to accumulated in the coastal area (Zhang et al., 2020), leading to their rapid input into sediments as shown in core SS2. Meanwhile, microplastics may sink more easily into sediments through gravitational differentiation, aggregation and biofouling under the low-energy stable environment in core SS2 (Mao et al., 2020). As revealed in our samples, more than 30% of microplastics belong to low-density polymers (mainly PP and PE), which confirms the occurrence of buoyancy modification via biofouling and aggregation.

4.3. Potential environmental impact of microplastics

New achievements have demonstrated a growing hazardous impact of microplastics for organisms with decreasing size (Nguyen et al., 2019), because smaller microplastics not only are more easily ingested, but also possess higher abilities to absorb toxic chemicals from the surrounding seawater. Möller et al. (2020) have proposed that the environmental impact of microplastics is most probably dependent on the abundance of their bioavailable fraction in the ecosystem. In this study, the high abundances of fine-grained microplastics (<100 μm) in surface sediments have been revealed in the coastal area of the ECS, which poses a potential threat to the benthic communities. Even worse, based on the increasing tendency of microplastic accumulation in cores DH3-1 and SS2, the abundances of fine-grained microplastics are also predicted to increase in the future. So do their ecological risks. Previous studies have already observed the ingestion of microplastics in benthic species in the ECS, and have suggested a high potential of microplastic accumulation in species at higher trophic levels through food chains (Su et al., 2019; Zhang et al., 2019b). To comprehend the impact of microplastics in the ECS, the concentrations of small microplastic particles in biota should be continuously monitored, and their ecotoxicological effect should be further verified.

4.4. Microplastics as a hidden part of sedimentary carbon storage

The impact of microplastics on carbon cycling has attracted attention from global investigators only very recently (Chen et al., 2018; Rillig, 2018; Romera-Castillo et al., 2018; Rillig and Lehmann, 2020). However, few studies have quantitatively evaluated the effect of microplastics on carbon storage, whatever regionally or globally. In this work, a novel method was adopted to determine the MPC contents in two cores from the inner shelf of the ECS for assessing the contribution of microplastics to the sedimentary carbon pool. Our results have revealed that the MPC contents occupy insignificant TOC proportions in sediments, only with a mean of 0.18% for cores DH3-1 and SS2, indicating an ignorable contribution to carbon burial. Based on the MPC/TOC ratios over a span of 43 years in core SS2, an exponential curve is yielded ($r = 0.9460$ and $p < 0.05$) (Fig. 5), suggesting that the contribution of microplastics to carbon storage in the topmost sediments in core SS2 will reach 3.39% and 6.80% in 2020 AD and 2025 AD, respectively. By then we have to calibrate such a significant microplastic contribution when estimating the annual carbon sequestration in marine sediments.

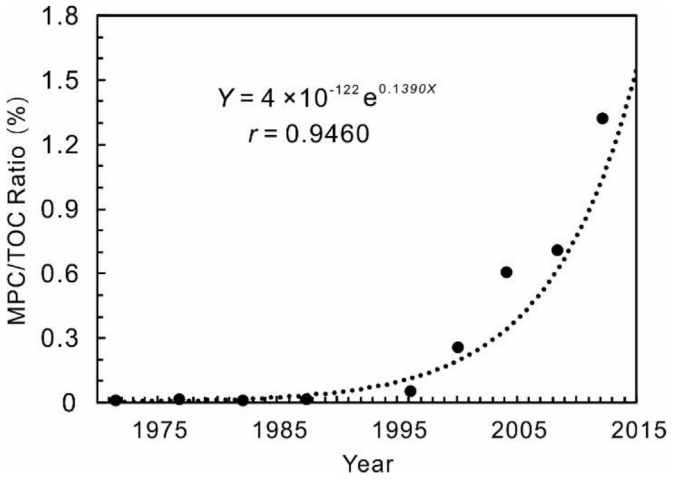

Fig. 5. Variation of the MPC/TOC ratios in sediment core SS2 over a span of 43 years (1971–2014 AD).

5. Conclusions

Two effective methods were adopted to measure the abundances of microplastics in two continuously deposited sediment cores for identifying the historical variation of microplastic accumulation, and quantitatively evaluating their contribution to carbon storage in the inner shelf of the ECS. Our results have disclosed a multidecadal increasing accumulation of microplastics in the sediment cores since the 1960s. We consider that microplastic accumulation along the coastal sediment zone in the ECS is closely associated with the rapid growth of plastic production and consumption under the background of oceanographic dynamics. Despite microplastics have made an inconsequential contribution (only 0.18%) to marine carbon burial in the past several decades, the contribution in surface sediments could increase to 3.4%–6.8% by 2025 AD with their continuous accumulation.

Credit author statement

Conceived and designed the experiments: J.H. Wang and Q. Zhu; Sampling: Q. Zhu; Performed experiments: J. Lin, B.Y. Yue, X.P. Xu, and X.M. Xu; Data processing and assessment: J. Lin, X.M. Xu, B.Y. Yue, and J. Liu; Wrote the paper: J. Lin and J.H. Wang; and Modified the manuscript: J.H. Wang. All authors approved the final version of this work.

Declaration of competing interest

The authors declare that they have no known competing financial interests or personal relationships that could have appeared to influence the work reported in this paper.

Acknowledgements

This work was financially supported by the Natural Science Foundation of Guangdong Province (Grant No. 18zxxt31), the National Natural Science Foundation of China (Grant Nos. 41703043 and 41673066), the National Basic Research Program of China (No. 2012CB956004), and the National Oil and Gas Major Project (2017ZX05008-002-050).

Appendix A. Supplementary data

Supplementary data to this article can be found online at https://doi.org/10.1016/j.chemosphere.2020.128658.

References

Akhbarizadeh, R., Moore, F., Keshavarzi, B., Moeinpour, A., 2017. Microplastics and potentially toxic elements in coastal sediments of Iran's main oil terminal (Khark Island). Environ. Pollut. 220 (Pt A), 720–731.
Alomar, C., Estarellas, F., Deudero, S., 2016. Microplastics in the Mediterranean Sea: deposition in coastal shallow sediments, spatial variation and preferential grain size. Mar. Environ. Res. 115, 1–10.
Bagheri, T., Gholizadeh, M., Abarghouei, S., Zakeri, M., Hedayati, A., Rabaniha, M., Aghaeimoghadam, A., Hafezieh, M., 2020. Microplastics distribution, abundance and composition in sediment, fishes and benthic organisms of the Gorgan Bay, Caspian Sea. Chemosphere 257, 127201.
Brandon, J.A., Jones, W., Ohman, M.D., 2019. Multidecadal increase in plastic particles in coastal ocean sediments. Sci. Adv. 5, eaax0587.
Browne, M.A., Crump, P., Nivem, S.J., Teuten, E., Tonkin, A., Galloway, T., Thompson, R., 2011. Accumulation of microplastic on shorelines worldwide: sources and sinks. Environ. Sci. Technol. 45 (21), 9175–9179.
Browne, M.A., Galloway, T.S., Thompson, R.C., 2010. Spatial patterns of plastic debris along estuarine shorelines. Environ. Sci. Technol. 44, 3404–3409.
Chen, C.S., Le, C., Chiu, M.H., Chin, W.C., 2018. The impact of nanoplastics on marine dissolved organic matter assembly. Sci. Total Environ. 634, 316–320.
Cole, M., Lindeque, P., Fileman, E., Halsband, C., Galloway, T.S., 2015. The impact of polystyrene microplastics on feeding, function and fecundity in the marine copepod *Calanus helgolandicus*. Environ. Sci. Technol. 49 (2), 1130–1137.
Comnea-Stancu, I.R., Wieland, K., Ramer, G., Schwaighofer, A., Lendl, B., 2017. On the identification of rayon/viscose as a major fraction of microplastics in the marine environment: discrimination between natural and manmade cellulosic fibers using Fourier transform infrared spectroscopy. Appl. Spectrosc. 71 (5), 939–950.
Eriksen, M., Mason, S., Wilson, S., Box, C., Zellers, A., Edwards, W., Farley, H., Amato, S., 2013. Microplastic pollution in the surface water of the laurentian great lakes. Mar. Pollut. Bull. 77, 177–182.
Fan, Y.J., Zheng, K., Zhu, Z.W., Chen, G.S., Peng, X.Z., 2019. Distribution, sedimentary record, and persistence of microplastics in the Pearl River catchment, China. Environ. Pollut. 251, 862–870.
Fischer, M., Scholz-Böttcher, B.M., 2017. Simultaneous trace identification and quantification of common types of microplastics in environmental samples by pyrolysis-gas chromatography-mass spectrometry. Environ. Sci. Technol. 51 (9), 5052–5060.
Hanvey, J.S., Lewis, P.J., Lavers, J.L., Crosbie, N.D., Pozo, K., Clarke, B.O., 2017. A review of analytical techniques for quantifying microplastics in sediments. Anal. Meth. 9 (9), 1369–1383.
Hossain, M.S., Rahman, M.S., Uddin, M.N., Sharifuzzaman, S.M., Chowdhury, S.R., Sarker, S., Chowdhury, M.S.N., 2020. Microplastic contamination in penaeid shrimp from the northern Bay of bengal. Chemosphere 238, 124688.
Isobe, A., Uchida, K., Tokai, T., Iwasaki, S., 2015. East Asian seas: a hot spot of pelagic microplastics. Mar. Pollut. Bull. 101, 618–623.
Jiang, Y., Yang, F., Zhao, Y.N., Wang, X., Chen, M., Wang, J., 2020. Abundance and characteristics of microplastics in the bellingshausen sea, Antarctica, are distinguished by the southern antarctic circumpolar current front. Chemosphere. https://doi.org/10.1016/j.chemosphere.2020.127653.
Jovanović, B., 2017. Ingestion of microplastics by fish and its potential consequences from a physical perspective. Integrated Environ. Assess. Manag. 13 (3), 510–515.
Law, K.L., Thompson, R.C., 2014. Microplastics in the seas. Science 345 (6193), 144–145.
Li, J.J., Huang, W., Xu, Y.J., Jin, A.M., Zhang, D.D., Zhang, C.F., 2020. Microplastics in sediment cores as indicators of temporal trends in microplastic pollution in Andong salt marsh, Hangzhou Bay, China. Reg. Stud. Mar. Sic. 35, 101149.
Lin, J., Xu, X.M., Chen, Y., Zhou, Q.Z., Yuan, L.R., Zhu, Q., Wang, J.H., 2019. Distribution and composition of suspended matters in the wintertime in the East China Sea. Sci. Total Environ. 664, 322–333.
Lin, J., Zhu, Q., Hong, Y.H., Yuan, L.R., Liu, J.Z., Xu, X.M., Wang, J.H., 2018. Synchronous response of sedimentary organic carbon accumulation on the inner shelf of the East China Sea to the water impoundment of Three Gorges and Gezhouba Dams. J. Oceanol. Limnol. 36 (1), 153–164.
Liu, S.F., Shi, X.F., Liu, Y.G., Zhu, A.M., Yang, G., 2009. Sedimentation rate of mud area in the East China Sea inner continental shelf. Mar. Geol. Quat. Geol. 29 (6), 1–7 (in Chinese).
Ma, Z.F., Jiang, W.J., Yang, S., 2019. China plastics industry (2018). China Plastics 33 (6), 127–146 (in Chinese).
Mao, Y.F., Li, H., Gu, W.K., Yang, G.F., Liu, Y., He, Q., 2020. Distribution and characteristics of microplastics in the Yulin River, China: role of environmental and spatial factors. Environ. Pollut. 265, 115033.
Martin, J., Lusher, A., Thompson, R.C., Morley, A., 2017. The deposition and accumulation of microplastics in marine sediments and bottom water from the Irish continental shelf. Sci. Rep. 7 (1), 10772.
Mathalon, A., Hill, P., 2014. Microplastic fibers in the intertidal ecosystem surrounding Halifax harbor, nova scotia. Mar. Pollut. Bull. 81, 69–79.

Matsuguma, Y., Takada, H., Kumata, H., Kanke, H., Sakurai, S., Suzuki, T., Itoh, M., Okazaki, Y., Boonyatumanond, R., Zakaria, M.P., Weerts, S., Newman, B., 2017. Microplastics in sediment cores from Asia and Africa as indicators of temporal trends in plastic pollution. Arch. Environ. Contam. Toxicol. 73 (2), 230–239.
Mintenig, S.M., Int-Veen, I., L€oder, M.G.J., Primpke, S., Gerdts, G., 2017. Identification of microplastic in effluents of waste water treatment plants using focal plane array-based micro-Fourier-transform infrared imaging. Water Res. 108, 365–372.
Möller, J.N., Löder, M.G.J., Laforsch, C., 2020. Finding microplastics in soils: a review of analytical methods. Environ. Sci. Technol. 54 (4), 2078–2090.
Nel, H.A., Dalu, T., Wasserman, R.J., Hean, J.W., 2019. Colour and size influences plastic microbead underestimation, regardless of sediment grain size. Sci. Total Environ. 655, 567–570.
Nguyen, B., Claveau-Mallet, D., Hernandez, L.M., Xu, E.G., Farner, J.M., Tufenkji, N., 2019. Separation and analysis of microplastics and nanoplastics in complex environmental samples. Acc. Chem. Res. 52 (4), 858–866.
Nor, N.H., Obbard, J.P., 2014. Microplastics in Singapore's coastal mangrove ecosystems. Mar. Pollut. Bull. 79 (1–2), 278–283.
Pang, C.G., Li, K., Hua, D.X., 2016. Net accumulation of suspended sediment and its seasonal variability dominated by shelf circulation in the Yellow and East China Seas. Mar. Geol. 371, 33–43.
Peng, G.Y., Zhu, B.S., Yang, D.Q., Su, L., Shi, H.H., Li, D.J., 2017. Microplastics in sediments of the Changjiang estuary, China. Environ. Pollut. 225, 283–290.
Phuong, N.N., Poirier, L., Lagarde, F., Kamari, A., Zalouk-Vergnoux, A., 2018. Microplastic abundance and characteristics in French Atlantic coastal sediments using a new extraction method. Environ. Pollut. 243 (Pt A), 228–237.
Prata, J.C., Castro, J.L., da Costa, J.P., Duarte, A.C., Rocha-Santos, T., Cerqueira, M., 2020. The importance of contamination control in airborne fibers and microplastic sampling: experiences from indoor and outdoor air sampling in Aveiro. Portugal. Mar. Pollut. Bull. 159, 111522.
Qiu, Q.G., Peng, J.P., Yu, X.B., Chen, F.C.Z., Wang, J.D., Dong, F.Q., 2015. Occurrence of microplastics in the coastal marine environment: first observation on sediment of China. Mar. Pollut. Bull. 98, 274–280.
Rillig, M.C., 2018. Microplastic disguising as soil carbon storage. Environ. Sci. Technol. 52 (11), 6079–6080.
Rillig, M.C., Lehmann, A., 2020. Microplastic in terrestrial ecosystems. Science 368 (6498), 1430–1431.
Rochman, C.M., Hoh, E., Kurobe, T., Teh, S.J., 2013. Ingested plastic transfers hazardous chemicals to fish and induces hepatic stress. Sci. Rep. 3, 3263.
Romera-Castillo, C., Pinto, M., Langer, T.M., Alvarez-Salgado, X.A., Herndl, G.J., 2018. Dissolved organic carbon leaching from plastics stimulates microbial activity in the ocean. Nat. Commun. 9, 1430.
Sagawa, N., Kawaai, K., Hinata, H., 2018. Abundance and size of microplastics in a coastal sea: comparison among bottom sediment, beach sediment, and surface water. Mar. Pollut. Bull. 133, 532–542.
Schuur, E.A.G., McGuire, A.D., Schädel, C., Grosse, G., Harden, J.W., Hayes, D.J., Hugelius, G., Koven, C.D., Kuhry, P., Lawrence, D.M., Natali, S.M., Olefeldt, D., Romanovsky, V.E., Schaefer, K., Turetsky, M.R., Treat, C.C., Vonk, J.E., 2015. Climate change and the permafrost carbon feedback. Nature 520 (7546), 171–179.
Seyoum, A., Pradhan, A., 2019. Effect of phthalates on development, reproduction, fat metabolism and lifespan in *Daphnia magna*. Sci. Total Environ. 654, 969–977.
Song, G.T., 1993. Production of plastics and its demand in China. Mod. Chem. Ind. 8 (5), 28–30 (in Chinese).
Stark, M., 2019. Letter to the editor regarding "Are We Speaking the Same Language? recommendations for a definition and categorization framework for plastic debris. Environ. Sci. Technol. 53 (9), 4677–4677.
Su, L., Deng, H., Li, B.W., Chen, Q.Q., Pettigrove, V., Wu, C.X., Shi, H.H., 2019. The occurrence of microplastic in specific organs in commercially caught fishes from coast and estuary area of east China. J. Hazard Mater. 365, 716–724.
Su, L., Sharp, S.M., Pettigrove, V.J., Craig, N.J., Nan, B.X., Du, F.N., Shi, H.H., 2020. Superimposed microplastic pollution in a coastal metropolis. Water Res. 168, 115140.
Suaria, G., Achtypi, A., Perold, V., Lee, J.R., Pierucci, A., Bornman, T.G., Aliani, S., Ryan, P.G., 2020. Microfibers in oceanic surface waters: a global characterization. Sci. Adv. 6 (23), eaay8493.
Talley, L.D., Feely, R.A., Sloyan, B.M., Wanninkhof, R., Baringer, M.O., Bullister, J.L., Carlson, C.A., Doney, S.C., Fine, R.A., Firing, E., Gruber, N., Hansell, D.A., Ishii, M., Johnson, G.C., Katsumata, K., Key, R.M., Kramp, M., Langdon, C., Macdonald, A.M., Mathis, J.T., McDonagh, E.L., Mecking, S., Millero, F.J., Mordy, C.W., Nakano, T., Sabine, C.L., Smethie, W.M., Swift, J.H., Tanhua, T., Thurnherr, A.M., Warner, M.J., Zhang, J., 2016. Changes in ocean heat, carbon content, and ventilation: a review of the first decade of GO-SHIP global repeat hydrography. Ann. Rev. Mar. Sci. 8, 185–215.
Thompson, R.C., Olsen, Y., Mitchell, R.P., Davis, A., Rowland, S.J., John, A.W.G., McGonigle, D., Russell, A.E., 2004. Lost at sea: where is all the plastic? Science 304 (5672), 838.
Turner, A., Holmes, L.A., 2015. Adsorption of trace metals by microplastic pellets in fresh water. Environ. Chem. 12 (5), 600–610.
Turner, S., Horton, A.A., Rose, N.L., Hall, C., 2019. A temporal sediment record of microplastics in an urban lake, London, UK. J. Paleolimnol. 61, 449–462.
Vianello, A., Boldrin, A., Guerriero, P., Moschino, V., Rella, R., Sturaro, A., Da Ros, L., 2013. Microplastic particles in sediments of Lagoon of Venice, Italy: first observations on occurrence, spatial patterns and identification. Estuar. Coast Shelf Sci. 130, 54–61.
Wang, J., Wang, M.X., Ru, S.G., Liu, X.S., 2019. High levels of microplastic pollution in the sediments and benthic organisms of the South Yellow Sea, China. Sci. Total Environ. 651, 1661–1669.
Wang, J.H., Xiao, X., Zhou, Q.Z., Xu, X.M., Zhang, C.X., Liu, J.Z., Yuan, D.L., 2018. Rates and fluxes of century-scale carbon storage in the fine-grained sediments from the central South Yellow Sea and Min-Zhe belt, East China Sea. J. Oceanol. Limnol. 36 (1), 139–152.
Wang, Z., Wagner, J., Ghosal, S., Bedi, G., Wall, S., 2017. SEM/EDS and optical microscopy analyses of microplastics in ocean trawl and fish guts. Sci. Total Environ. 603–604, 616–626.
Willis, K.A., Eriksen, R., Wilcox, C., Hardesty, B.D., 2017. Microplastic distribution at different sediment depths in an urban estuary. Front. Mar. Sci. 4, 419.
Woodall, L.C., Sanchez-Vidal, A., Canals, M., Paterson, G.L., Coppock, R., Sleight, V., Calafat, A., Rogers, A.D., Narayanaswamy, B.E., Thompson, R.C., 2014. The deep sea is a major sink for microplastic debris. Roy. Soc. Open Sci. 1 (4), 140317.
Xu, X.M., Zhu, Q., Zhou, Q.Z., Liu, J.Z., Yuan, J.P., Wang, J.H., 2018. An improved method for quantitatively measuring the sequences of total organic carbon and black carbon in marine sediment cores. J. Oceanol. Limnol. 36 (1), 105–113.
Xue, B.M., Zhang, L.L., Li, R.L., Wang, Y.H., Guo, J., Yu, K.F., Wang, S.P., 2020. Underestimated microplastic pollution derived from fishery activities and "hidden" in deep sediment. Environ. Sci. Technol. 54 (4), 2210–2217.
Yu, F., Yang, C.F., Zhu, Z.L., Bai, X.T., Ma, J., 2019. Adsorption behavior of organic pollutants and metals on micro/nanoplastics in the aquatic environment. Sci. Total Environ. 694, 133643.
Zhang, C.F., Zhou, H.H., Cui, Y.Z., Wang, C.S., Li, Y.H., Zhang, D.D., 2019a. Microplastics in offshore sediment in the Yellow Sea and east China sea, China. Environ. Pollut. 244, 827–833.
Zhang, F., Wang, X.H., Xu, J.Y., Zhu, L.X., Peng, G.Y., Xu, P., Li, D.J., 2019b. Food-web transfer of microplastics between wild caught fish and crustaceans in East China Sea. Mar. Pollut. Bull. 146, 173–182.
Zhang, Z.W., Wu, H., Peng, G.Y., Xu, P., Li, D.J., 2020. Coastal ocean dynamics reduce the export of microplastics to the open ocean. Sci. Total Environ. 713, 136634.
Zhao, J.M., Ran, W., Teng, J., Liu, Y.L., Liu, H., Yin, X.N., Cao, R.W., Wang, Q., 2018. Microplastic pollution in sediments from the bohai Sea and the Yellow Sea, China. Sci. Total Environ. 640–641, 637–645.
Zheng, Y.F., Li, J.X., Cao, W., Liu, X.H., Jiang, F.H., Ding, J.F., Yin, X.F., Sun, C.J., 2019. Distribution characteristics of microplastics in the seawater and sediment: a case study in Jiaozhou Bay, China. Sci. Total Environ. 674, 27–35.
Zhu, L., Bai, H.Y., Chen, B.J., Sun, X.M., Qu, K.M., Xia, B., 2018. Microplastic pollution in north Yellow Sea, China: observations on occurrence, distribution and identification. Sci. Total Environ. 636, 20–29.
Zhu, X., Nguyen, B., You, J.B., Karakolis, E., Sinton, D., Rochman, C., 2019. Identification of microfibers in the environment using multiple lines of evidence. Environ. Sci. Technol. 53 (20), 11877–11887.